Published in final edited form as:
J Phys Chem B. 2011 October 13; 115(40): 11718–11726. doi:10.1021/jp203292h.

Methionine ligand lability in bacterial monoheme cytochromes *c*: an electrochemical study

Benjamin D. Levin[1], **Mehmet Can**[2], **Sarah E. J. Bowman**[2], **Kara L. Bren**[2], and **Sean J. Elliott**[1,*]

[1]Department of Chemistry, Boston University, 590 Commonwealth Avenue, Boston, MA 02215

[2] Department of Chemistry, University of Rochester, Rochester, NY 14627

Abstract

The direct electrochemical analysis of adsorbed redox active proteins has proven to be a powerful technique in biophysical chemistry, frequently making use of the electrode material pyrolytic "edge-plane" graphite. However many heme-bearing proteins such as cytochromes *c* have been also examined systematically at alkanethiol-modified gold surfaces, and previously we have reported the characterization of the redox properties of a series of bacterial cytochromes *c* in a side-by-side comparison of carbon and gold electrode materials. In our prior findings we reported an unanticipated, low potential (E_m ~ -100 mV vs SHE) redox couple that could be analogously observed when a variety of monoheme cytochromes *c* are adsorbed onto carbon-based electrodes. Here we demonstrate that our prior phenomological data can be understood quantitatively in the loss of the methionine ligand of the heme iron, using the cytochrome *c* from *Hydrogenbacter thermophilum* as a model system. Through the comparison of wild-type protein with M61H and M61A mutants, in direct electrochemical analyses conducted as a function of temperature and exogenous ligand concentration, we are able to show that Met-ligated cytochromes *c* have a propensity to lose their Met ligand at graphite surfaces, and that energetics of this process (6.3 ± 1 kJ/mol) is similar the energies associated with "foldons" of known protein folding pathways.

Keywords

Pseudomonas aeruginosa; *Hydrogenobacter thermophilus*; cytochrome *c*; protein film voltammetry

INTRODUCTION

Iron-protoporphyrin IX (heme) containing proteins occupy vast and diverse areas of biological function, where the heme cofactor frequently acts as an electron transfer element functioning in respiration, catalysis, and signaling. The ubiquitous nature, robust structure and spectroscopic signatures of heme proteins are the traits that have driven these proteins to be amongst the most studied biomolecules. Folding, dynamics, and function of the various proteins have prompted analyses through the sequence-structure-function paradigm,[1-4] where the functional characterization of individual proteins is often described by the heme Fe(III/II) redox potential (E_m). Several factors have been strongly implicated in controlling the potential, particularly axial ligation and the second sphere interactions such as hydrogen-

* To whom correspondence should be addressed. Address: Department of Chemistry, Boston University, 599 Commonwealth Avenue, Boston, MA 02215. elliott@bu.edu tel: 617-358-2816 FAX: 617-353-6466.

Supporting Information. Additional voltammetric data for native and M61A mutant. This material is available free of charge via the Internet at http://pubs.acs.org

bonding and solvation:[5-9] in such models, E_m is coarsely determined by the axial coordination and further tuned by secondary interactions upon the axial ligands and heme pocket environment.[5,11-15] Cytochromes *c* (cyts *c*) are additionally complex due to the covalent attachment of the porphyrin ring to the protein backbone through two thioether linkages in a -Cys-X-X-Cys-His- binding motif, where the histidine (His) serves as the proximal heme ligand,[8,10] while a potential sixth ligand (such as a distal methionine (Met)) is donated from elsewhere in the protein scaffold. Here we consider the *Hydrogenobacter thermophilus* (Ht) cytochome c_{552}, which displays a canonical cyt *c* fold (Figure 1);[8,10,16] Ht cyt c_{552} and its variants have been characterized extensively to further develop an understanding of how the heme attachment motif and heme pocket residues affect midpoint potential and dynamic properties.[11-15,17-21] In this report, we utilize the Ht cytochrome as a model system for the assessment of redox thermodynamics and changes in midpoint potential associated with the loss of the Met ligand.

Recent electrochemical investigation of bacterial cytochromes *c* by protein film voltammetry (PFV) revealed not only the Fe(III/II) potential of the typical His/Met-bound form of the active site, but a second electrochemical equilibrium, which could be detected as a function of electrode material.[13] While Ht cyt c_{552} as well as the *Pseudomonas aeruginosa* (Pa) cytochrome c_{551} exhibit a single electrochemical feature when adsorbed onto modified-gold electrodes (Au-SAM electrodes),[14] a second reversible couple at approximately -100 mV (vs hydrogen at pH 7) was observed upon pyrolytic graphite edge (PGE) electrodes (Figure 2), a phenomenon that has been now confirmed for a small number of bacterial *c*-type cytochromes.[22] The second redox couple was found to be due to a species that was best described as a locally-unfolded, or “Met-loss” state, via comparisons with chemically unfolded protein[13] and correlation of the yield of the Met-loss form with thermal loss of intensity of a 695-nm absorption feature in the optical spectra of the cytochromes studied.[14] Interrogation of the Met-Fe(III/II) interaction[31-35] and the structural implication Met displacement[23,36-39] have underpinned the interplay between global and local environment in controlling the redox potential and thermodynamics. Superficially, the loss of Met as a ligand in the bacterial cyts *c* may be analogous to the changes observed in mitochondrial cyts *c* at high pH values,[23-26] i.e., the so-called “alkaline transition” which is marked by a replacement of the distal Met ligand with a nitrogenous base (typically one of three lysine residues contained within the methionine donating loop of the protein scaffold[17,27-30]) but an overall retention of global structure.[23,36] In contrast, cytochrome c_2 proteins from purple bacteria contain axial Met as a ligand, but with additional “hinge-like” regions on either side of the methionine-bearing loop, allowing for the protein structure to be largely unaffected by the local conformational changes resulting from small molecule binding.[37,40-42] Similarly, alkaline-like conformational changes have been demonstrated in the presence of membrane phospholipids, where interaction of cardiolipin with the solvent exposed heme propionates has been implicated in stimulating conformational changes and the lowering of E_m by several hundred millivolts.[38,39,43-45]

However, the analogy to the alkaline transition fails in the case of our prior reporting of an electrochemically detected “Met-loss” state, as the bacterial homologs of mitochondrial cytochrome *c* all lack the analogous Lys residues that might serve as ligands. Critically, by all estimates, the resulting shift in heme iron coordination synonymous with the alkaline transition yields a new state that possesses a reduction potential even lower in potential[5,13,24-26,45-47] than that which we and others have reported for bacterial cytochromes *c* upon PGE electrodes.[13,22] While previous efforts to characterize loop- and ligand-reorganization of Met-ligated cyts *c* have correlated global stability with maintenance of Met-Fe coordination (using thermal denaturation experiments coupled to NMR and optical techniques),[48-50,51] here we further our prior studies of the link between protein

dynamics and loss of the Met-ligand in bacterial cyts *c* through the technique of direct electrochemistry.

Presently we have conducted a systematic, variable-temperature, and ligand-binding electrochemical study to interrogate the low potential Met-loss feature associated with the bacterial Htcyt c on PGE electrodes. Mutation of the axial methionine to alanine or histidine has allowed us to impose specific coordination of the heme-porphyrin moiety. We have utilized protein film voltammetry (PFV) to directly report upon relative populations of Met-ligated and Met-loss forms. Midpoint potentials agree well with models and similar mutations from other cyts *c*.[5,26,34,52-54] Temperature-dependent voltammetry has allowed the comparison of enthalpy and entropy for both the normal and alkaline forms of various cytochromes. Redox thermodynamics of our system correlate well with previously reported values which serve as further validation for our findings.[26,46,47,49,53,55] Additionally, as a result of having two distinct populations on a single surface we were able to determine the Gibbs free energy for the conformational change. Small molecule binding has been used to inform on the relative accessibility of the heme, which further elucidate the relationship between structure and the redox chemistry in the context of the lability of the Met61 ligand.

MATERIALS AND METHODS

Protein Production and Purification

The mutation M61H was prepared by the polymerase chain overlap extension method.[56] The mutation M61H was prepared by QuikChange XL site directed mutagenesis Kit (Stratagene). pSCH552 was used as the DNA template and 5' GGG GTT CTG TTC CCC ACC CTC CTC AAA ATG TAA CCG ATG CG 3' and 5' CGC ATC GGT TAC ATT TTG AGG AGG GTG GGG AAC AGA ACC CC 3', were used as forward and reverse mutagenic primers, repectively. Overexpression was achieved by *E. coli* BL21(DE3) culture containing the appropriate pSCH552 plasmid and pEC86, containing the cytochrome *c* maturation genes *ccmABCDEFGH*.[57] Expression of protein samples and purification procedures of Ht cyt *c* and mutants, M61A and M61H, were as previously described. [58,59]

Electrochemical Methods

All PFV measurements were carried out on a PGSTAT30 AutoLab (Ecochemie) electrochemical analyzer equipped with FRA and ECD modules. A water-jacketed glass cell was used in a three electrode configuration. Cell temperature was maintained by refrigerating circulator. A resin-body calomel electrode (Accumet) and platinum wire were used as the reference and counter electrodes respectively. The calomel reference was maintained at a constant temperature (293 ± 0.5 K). Potentials are reported vs. standard hydrogen electrode (SHE) and corrected by +242 mV. Nonfarrodaic (charging) components of the resulting voltammograms were removed through polynomial baseline subtraction. Regular electrochemical noise was suppressed through Fast Fourier Transformation. Data analysis was done utilizing the open source program SOAS.[60]

Pyrolyitic edge-plane graphite (PGE), or polycrystalline gold wire (2.0 mm diameter) embedded in resin served as the working electrode. The gold electrodes were polished with successively finer grits of alumina (1.0, 0.3, 0.05 μM, Buehler). Final electrochemical cleaning was carried out in 0.1 M H_2SO_4 by cycling 0.2 – 1.35 V (vs SCE). Cleaned surfaces were modified in an 0.5-2 mM ethanolic solution of 6-mercaptohexanol for 12 hours. Excess alkane thiol was removed by rinsing with ethanol followed by water and then considered ready for use. PGE electrodes were polished with aqueous 1μ alumina slurry, followed by sonication. Protein films were generated on both surfaces by directly applying 2 μL cytochrome *c*. Excess protein was washed away with a small amount of cold buffer.

Thermodynamics of electron transfer was interrogated by variable-temperature experiments over a limited range of temperatures (0 – 65°C). Reaction entropy $\left(\Delta S^{\circ\prime}_{rc}\right)$ for the Fe (III/II) couple may be determined by the relation:

$$\Delta S^{\circ\prime}_{rc}=\Delta S^{\circ\prime}_{red}-\Delta S^{\circ\prime}_{ox}=nF\left(\frac{dE^{o\prime}}{dT}\right) \quad (1)$$

With the assumption that $\Delta S^{\circ\prime}_{rc}$ is constant over the temperature range investigated, the slope of the E_m versus T should be linear and equal to $\Delta S^{\circ\prime}_{rc}$. Enthalpic change may be obtained based on the previous assumption. From the Gibbs-Helmholtz equation, $\Delta H^{\circ\prime}_{rc}$ may be extracted form the negative slope of an E_m/T versus 1/T plot.

The populations of Met-loss and normal forms of Ht cyt *c* are represented in one of two ways: either as the peak area (total charge passed) for each of the two redox couples, or as a quantity proportional to the peak height of each redox couple in a CV. The peak height formalism for an anodic (oxidation, i_{pa}) or cathodic (reduction, i_{pc}) feature is shown in equation 2.[61]

$$i_p=\frac{n^2F^2A\Gamma\nu}{4RT} \quad (2)$$

Here, n is the number of electrons, F is the Farraday constant, R is the ideal gas constant, T is the temperature, A the physical surface area, Γ total electroactive coverage, and scan rate ν. For a process with n=1, the population is directly proportional to the observed current. Temperature dependent behavior may be assessed using the equilibrium form of the Gibbs free energy equation and linear form of the van't Hoff equation (equation 3):

$$\ln K_{eq}=-\frac{\Delta H^{\circ}}{RT}+\frac{\Delta S^{\circ}}{T} \quad (3)$$

The equilibrium constant K_{eq} may be determined at each temperature by the ratio of Met-loss to normal form, and a plot of $\ln(K_{eq})$ versus T^{-1} allows the extraction of the thermodynamic parameters. Here we assessed K_{eq} in terms of both the peak area and peak height of each redox couple. $\Delta G°$ values were calculated at 298K.

Imidazole binding studies were carried out in 50 mM phosphate/citrate buffer, pH 6.0, containing varying amounts of imidazole (0 – 1 M). Electrodes with protein films were maintained in chilled buffer between measurements. All buffers were purged of oxygen with argon prior to measurement. Determination of the association constants for imidazole (K_a) were conducted in the manner of Sutin and Yandell. [62]

RESULTS

We have continued our previous work on the Ht cyt *c* protein as a model system for interrogating structure-function relationships that impact redox properties, such as the reduction potential. As in our prior efforts,[12-14] we have found that the Ht wild type (WT) protein, reproducibly gives excellent electrochemical responses at PGE electrodes; however, as observed previously, the Ht WT protein exhibits two one-electron features: the typical redox couple observed at +210 mV, and what we have called the “Met-loss” form at -110 mV (Figure 2). To probe the hypothesis that the minor component observed is indeed a

"Met-loss" state, and to interrogate whether other potential axial ligands might be present, we have prepared the M61A mutant, presuming that removal of the axial methionine by mutation to an alanine will provide an open coordination site that may be occupied by another exogenous ligand or, in the absence of exogenous small molecules, water/hydroxide may occupy the position of a sixth axial ligand. Importantly, the methionine donating loop of Ht does not contain another nitrogenous amino acid (*i.e.*, lysine) that could be poised to replace the thioether bond of methionine, as has been observed in eukaryotic cyts *c*.[16] At 0 °C the presence of the low-potential, Met-loss form is sufficiently suppressed such that nearly the entire electrochemical response is due to the normal form of the protein, observed at +210 mV (Figure 3A). Upon removal of M61 in the M61A mutant, we observe a single feature: a one-electron redox couple at the dramatically lower potential of -163 mV (Figure 3B). Similarly, electrochemical characterization of the M61H mutant similarly resulted in simple voltammetric responses that display a single redox couple (Figure 3C) with midpoint potential of -103 mV (and no indication of any additional features), as the M61H mutant is most likely a stable six-coordinate bis-His ligated heme. In all cases, there is a deviation from ideal electrochemical behavior of an adsorbed species: while all features appear symmetric and largely reversible, a significant (10-20 mV) peak separation is observed at 0 °C. In all cases, higher temperatures restored reversibility as peak separation tended toward zero, suggesting that at 0 °C a dispersed population of cytochrome *c* conformations were "frozen" on the PGE surface at low temperatures, giving a distribution of electron transfer rates and potentials that could be averaged out at higher temperatures. Notably, for all of these experiments the ratio of peak current (i_{pa}/i_{pc}) observed for each species is unity, over a wide range of scan-rates (from 20 mV/s to 20 V/s). Additionally we note that as a control, the electrochemistry of M61A electrochemistry was examined using mercapto-hexanol modified gold electrodes (Figure S1, as reported previously[12,14]), resulting in a single, reversible low-potential feature.

Ligand Binding

Upon the addition of imidazole (Im) to the cell solution a modulation of the peak height of the Ht cyt *c* voltammetric response was observed. The normal form decreased with a concurrent increase of a lower potential state, presumed to be an Im-bound form (Figure 4A). Midpoint potentials for the native and Im-bound forms are summarized in Table 1. At each concentration of ligand, approximately one minute was required to the system to come to equilibrium, and multiple cyclic voltammograms were collected until a stable signal was maintained. Ht M61A was also found to be sensitive to imidazole. While the ligand-free from of the mutant was found to have a reduction potential of -163 mV, Im adduct formation began at low (μM) concentrations of the ligand, and full conversion of the electrochemical response was attained at 5 mM Im, with a potential of -69 mV for the Ht M61A-Im complex (Figure 4B). Ht M61H has no change in peak position under any of the imidazole concentrations used in this study (Figure 4C). Imidazole binding was achieved in a concentration dependent manner for the WT and M61A mutants, and representative data of the increases in the voltammetric response due to adduct formation, and concomitant decreases in the ligand-free state, are illustrated in Figure 5. Binding constants for Im were estimated to be 417 ± 40 M^{-1} and 1323 ± 33 M^{-1} for Ht Wt (Figure S2) and M61A respectively. The binding of imidazole to cyt *c* films was found to be essentially kinetically irreversible on the time-scale of all electrochemical analyses. Electrodes used during the titration experiments were maintained in fresh electrochemical buffer, which was changed on a daily basis. Over the course of 5 days there was no change in the CV that could be attributed to a chemical change, while a small amount (less than 20%) of film loss was observed.

Redox thermodynamics

Variable temperature PFV was conducted to determine the thermodynamic parameters, $\Delta H^{\circ\prime}_{rc}$ and $\Delta S^{\circ\prime}_{rc}$, that contribute to the free energy of the redox reaction; these data are summarized in Table 2. Over the temperature regime studied (0 – 65°C) the E_m follows a linear trend, where the observed reduction potentials of the Ht WT protein (E_m + 210 mV at 0 °C) steadily decreased as the temperature increased. However, the potential of the "Met-loss" couple moves in a more positive direction as a function of increasing temperature. As noted above, both features of the Ht cyt *c* cyclic voltammogram become more reversible (peak separation decreases) as the temperature increases (Figure 6), and both WT proteins and M61H and M61A mutants showed little film loss until around 50°C, where film stability decreased. The temperature dependence of the reduction potential for Ht M61H and M61A are plotted along with those of native Ht *cyt* c in Figure 7 and Figure 8 shows the corresponding Gibbs Helmholtz plot. In every case, the data follow a linear change in reduction potential over the range studied, indicating that just one protein state is associated with the redox reactions studied at each couple. However, as the temperature was increased for the WT Ht protein, the Met-loss feature became more pronounced in terms of overall current, while the normal form decreased significantly. As the total area of each peak is equal to the total charge passed, and therefore the total population of the species engaged in a redox process occurring at that potential, either the electrochemical area or peak height can be used to calculate the relative amounts of each redox-active population. From those data, one can find the equilibrium constant (K_{eq}) for the conformational inter-conversion between the normal Met-bound and Met-loss states, as described in further detail below.

DISCUSSION

Previously we have reported unusual, low potential redox couples for bacterial cyts *c* adsorbed upon carbon-based electrodes, where the low-potential form was attributed to a so-called "Met-loss" state, which may be similar to the mitochondrial alkaline transition.[13] The alkaline transition is a phenomenon that has been examined primarily for mitochondrial cytochrome *c* and a large downward shift in redox potential is a key consequence of the alkaline conformational rearrangement.[26] Interestingly, neither Ht nor Pa cytochromes contain lysine residues within loop 3, the location that has been ascribed to nitrogenous bases that are poised to replace the axial Met in adopting the alkaline conformation. Further, generality of possible ligand displacement has for hemoproteins at PGE electrodes has been shown.[22] In comparison, the refolding of Pa cyt *c* studied by stopped flow kinetics additionally shows no evidence for a nitrogenous ligand rearrangement,[63] while horse heart cytochrome *c* (Hh cyt *c*) goes through at least two intermediate steps in the folding process where one is a bis-His coordinated species.[17] In order to elucidate the nature of the Met-loss feature,[13] we have examined mutations of the axial ligand methionine from Ht cyt *c,* and the impact on electrochemical potential and redox thermodynamics.

Site-Directed Mutants at Met61

Our initial probe of the low potential feature was the installation of histidine in the axial position, where we hoped to create a stable six coordinate heme. Therefore, in correspondence to the bis-His ligated cytochromes *c*,[64,65] it was not surprising that Ht M61H had a single electrochemical feature at a potential significantly lower than WT protein (Figure 3B). The assumed bis-His heme proved to be a reasonable facsimile to the native Met-loss feature, *i.e.,* within 7 mV. Similarly, installation of Ala at the Met61 position was designed to yield an open coordination site where water/hydroxide (depending on the pH), or an exogenous ligand could bind. Investigation of the Ht M61A mutant yielded similar results as M61H, however the single couple was significantly lower in redox

potential (Figure 3C and Table 1). Interestingly, these low potential species are still higher than those observed for the alkaline conformer of yeast iso-1-cyt *c*.[26,30]

Greater solvation of the heme pocket will likely contribute to the lowered midpoint potentials: Solvation effects have been correlated by Gray and Tezcan to account for the redox potential shifts due to heme encapsulation, where heme potentials can be tuned over a nearly 700mV window.[5] For structurally characterized *c*-type hemoproteins, the increase of solvent exposure significantly decreased the observed redox potential of the heme center. Here, the M61A mutation was designed to increase solvent access, and the reduction in E_m is severe (a reduction of roughly 300 mV with respect to wild-type); here the lowering of potential may not be as great as that observed by Gray and Tezcan due to interactions between the position-61 bearing loop and other structural elements. In contrast, the more negative reduction potential of Ht M61H compared to wild-type is likely the result of the new His sixth ligand donating a nitrogenous base.[66] Again there are no other potential ligand candidates within the Met-donating loop, and no other His residues exist within the protein except the distal heme ligand, His16.

Probing Met-loss Dynamics with Im binding

Exogenous ligand binding experiments have been used extensively to probe the electronic and physical characteristics of heme proteins.[67] The transient dissociation of the significantly weaker Met-Fe bond (as compared to either His or small molecules) allows for the binding of other peptide-based ligands or exogenous ligands such as imidazole, azide, cyanide, and pyridine, which will bind to the heme iron at the open sixth site of the heme.[31-35,42] The resulting ligand bound structures are not generally physiologically relevant, but provide information on local structure and dynamics of the heme environment. Previous ligand binding studies with mitochondrial sources showed that the strongest **π**-acceptors were also ones that preferred binding to Fe(II).[5,33] This generally supports the model that ferrous iron delocalizes 3d electrons into the **π**-orbitals of soft ligands, enhancing stability of Met-Fe(II) versus Fe(III).[33] To further probe the relative accessibility of the heme pocket and lability of the axial ligation, we have employed Im-binding as a means to reveal, remove, and replace the labile Met61 ligand. Previously we have demonstrated that Pa cyt *c* can bind Im when adsorbed at electrodes.[13] Figure 4 demonstrates that native Ht cytochrome and Ht M61A, have similar susceptibilities to form imidazole adducts that replace the axially coordinating ligand, while Ht M61H does not provide any electrochemical evidence for adduct formation. Imidazole is a good mimic for histidine ligation, which is supported by the structural analysis of Hh cyt *c*.[23] Formation of Ht cyt *c*-Im adducts for either the WT protein or M61A produce species that are electrochemically very similar, although not identical. Modulation of the peak intensities (i_p) for both forms, native and imidazole-bound, occurs in a concentration dependent manner (Figure 5). The similar nature of the redox potentials, support the idea that Im-binding and subsequent structural rearrangements tune the reduction potential coarsely, while secondary coordination sphere interactions (*e.g.*, hydrogen bonding and solvent interactions) further refine the midpoint that is observed.[5,24,25] The effects of the ligand binding are not only seen in the full length protein but also in models such as microperoxidases, the 6 to 11 amino acid long proteolyic products of mitochondrial cytochromes.[9,68] Binding of nitrogenous ligands to N-acetyl-microperoxidase-11 (AcMP11) decreases the overall reduction potential with respect to the water bound form. Furthermore the bulkier ligands result in the more pronounced decreases in reduction potential.[24] The association constants, K_a, for the Im adduct of both Ht and M61A are orders of magnitude greater than that observed for Hh cyt *c*.[62] Yet they are of a similar magnitude to those observed for *Rhodobacter sphaeroides* (Rs) and *Rhodobatcter capsulatus* (Rc) cytochrome c_2,[37,41] which contain additional “hinge-like” regions adjacent to the Met-bearing loop absent in either Ht

or Hh proteins. Perhaps more significant, the data collected here are all from an adsorbed mode, while prior efforts have monitored diffusion-based associations of Im and the cyt *c* of interest. Thus, while Ht appears to have an enhanced affinity for Im with respect to the Hh protein, this trait may be a reflection of the surface interactions between the protein scaffold and PGE, which result in an enhanced stability of the Met-loss state, and loop rearrangements that are required in that process.

Redox Thermodynamics and the Met-loss Equilibrium

We examined the redox thermodynamics of Ht cyt *c* and its Met61 mutants in order to understand the effects of our mutations on the fundamental driving force for the electron transfer process. Figure 6 depicts the typical electrochemical response with the change in temperature, resulting in redox thermodynamic parameters summarized in Table 2. Overall these values correspond similarly those described by both Sola and Gray for mitochondrial cytochromes, as well as heme microperoxidases.[24,46,53,54] A comparison of the entropic and enthalpic terms (Figures 7 and 8, Table 2), for the native and Met-loss conformers of Ht cyt *c,* indicate that while sign of $\Delta S^{\circ'}_{rc}$ has switched, the difference between redox potentials is still largely driven by differences in enthalpy, where the enthalpic contributions have been correlated to stabilization of the Fe(II) state.[5,24] Some small curvature was noted during the analysis of the alkaline form, however these are within error of the measurements. In several mitochondrial cases, clear linear breaks have been reported in the entropic and Gibbs-Helmholtz plots.[52] An interesting observation is the entropic loss for M61H, which displays a largest entropic contribution of the proteins studied here, and with a negative magnitude, suggestive of the decreases in $\Delta S°$ that have been observed for aqueous metal ions ($M^{2+/3+}$) and attributed to shielding by large organic ligands in aqueous environment.[70,71] Entropic/enthalpic compensative forces due to solvation are consistent here as well.[69] Notably, our data are in good general agreement with the magnitude of redox thermodynamic parameters measured by voltammetry utilizing semipermeable membranes for native HT, and mutations affecting electrostatic interactions of the N- and C- termini.[55,72,73] The comparison indicates that the M61 mutations have not overwhelmingly affected the intrinsic thermodynamics associated with the electron transfer for Ht cyt *c*.

An unexpected benefit from the temperature dependence of the Ht cyt *c* electrochemical data is observation of variable peak current intensity (i_p) of the normal and Met-loss forms over the temperature range investigated. As Figure 6 shows, the area and i_p for the two forms appear to be inversely correlated: as the temperature increases the percentage of normally folded Ht cyt *c* diminishes while the Met-loss form accumulates. We found these changes to be fully reversible by jumping the temperature, and that the population intensities rapidly equilibrated, ensuring that at each temperature the system was equilibrium. Additionally, we note that the equilibrium surface concentration of the two species cannot be due to pH-induced effects: as we have shown previously for the WT Ht protein, at pH 6.0, the midpoint potential is invariant as a function of pH. Thus, we could quantitatively assess the surface concentration of both states as a function of temperature, by using either i_p or the area of the electrochemical signature, and thereby we determined the equilibrium constant associated with the thermally driven conversion of the normal form to the Met-loss state.[25,46,47] In this way, we have been able to elaborate upon protein electrochemistry as a tool to examine the free energy associated with conformational changes ascribed to groups of residues that cooperatively interact, termed foldons, joining the ranks of hydrogen exchange mass spectrometry and NMR, which are more widely used to interrogate foldon thermodynamics.[74] The free energy of the alkaline transition (ΔG_{AT}) has been investigated electrochemically through the thermodynamic parameters (ΔS_{alk} and ΔH_{alk}) as a function of anapparent equilibrium constant (K_{app}).[46] And here, we can directly measure the normal and Met-loss populations as a function of temperature, using either the total current passed

associated with the individual redox couples (peak area) or simply the maximal height of the current response (i_p). Both of these attributes were used to calculate the equilibrium constant describing the conversion from normal form to the Met-loss state, (K_{ML}). And a subsequent plot of ln (K_{ML}) *vs.* T^{-1} (Figure 9) yields a straight line with slope of $-\Delta H^{\circ} / R$ and y-intercept $\Delta S^{\circ} / R$. The enthalpy for the conversion to the Met-loss state is 37.0 ± 0.2 kJ mol^{-1}, a value that is on par with the sub-global free energies of hydrogen exchange (ΔG_{HX}) and those determined for ΔG_{AT} from direct voltammetry.[25,47,53,74,76-81] However, utilizing the classic assumption that entropic term remains independent of temperature, we find that the Gibbs free energy (ΔG_{ML}) for the Met61 loss is 6.3 ± 0.1 kJ mol^{-1} at 273 K, indicating that entropy contributes substantially to the overall free energy of the conversion. While it is unclear whether the assumption of constant entropy and enthalpy over all temperatures is appropriate, Table 3 places these data in the context of free energies associated with other cytochrome *c* folding substructures, or foldons, as determined by hydrogen/deuterium exchange (ΔG_{HX}) or for the (ΔG_{AT}). Currently the foldon assignment of Ht cyt c_{552} is not available, however we note that the Met61-donating loop of the corresponding Hh and Pa proteins have very similar ΔG_{HX} values. While it is possible that our use of a van't Hoff plot to determine ΔG_{ML} has over-estimated the entropic contribution to the free energy, the enthalpic term is in excellent agreement with the energetics associated with localized unfolding for other cyts *c*. Yet the apparent overall lowering of free energy for loss of the Met ligand, when compared to the foldon energies measured for either Pa or Hh proteins or the free energy for the alkaline transition for YCC[47] or its mutants[25] (monitored by diffusional voltammetry at passivated gold electrodes), again likely reflect the difference in monitoring localized unfolding at a surface, versus free in solution. Indeed, it appears that PGE itself lowers the free energy requirements for loss of the Met ligand.

Again we can turn to the structural models for the local ligand dynamics in cyts *c* to provide some insight into the Met-loss state we observe here. In the case of the Rc and Rs cyts c_2, Dumortier and Cusanovich provide evidence that a local region flanking the axial ligand (Met 96, Rc numbering) facilitate different aspects of the isomeration.[37,40-42] Amino acid residues 93 and 95 in the Met-bearing loop assist the conversion of the closed to open form while residues 98 and 99 affect the imidazole affinity by providing better solvent access.[41] Thus spanning the entire region of residues 88-102, the behavior is akin to a “hinge”.[37,40-42] Yet, the first NMR model of the YCC alkaline form from Gray, Mauk, Bertini and coworkers demonstrated that rearrangement of the Met-donating loop is drastic, where there is a general increase in loop mobility, and an absence of other protein contacts aside from Lys73-Fe ligation.[36] Imidazole binding to horse heart cyt *c* similarly goes through substantial backbone reorganization for the residues around Met80 (the equivalent to Met61 in the bacterial proteins) to accommodate the new small molecule ligand. NMR models show that the plane of the bound imidazole is perpendicular to the distal histidine, and acts similar to a histidine ligand with respect to orientating the heme the magnetic properties.[23] These exemplify a key element of the Met-Fe coordination: the local structural dynamics play a crucial role in the maintenance of the coordination. In contrast, temperature dependent NMR and optical spectroscopy studies of bacterial cyt *c* orthologs (members of the cyt c_8, such as the Ht protein studied here) have been used to support a model where the maintenance of the Met-Fe(III) is linked to global, rather than local stability.[48,50] Thus, by using direct electrochemical analyses, we have demonstrated a previously underappreciated similarity between bacterial cyts c_8 and mitochondrial and cyts c_2, and bridged a gap in our understanding of the importance of localized unfolding in the stability of the Met-Fe(III) bond. The Met-loss form can be additionally informed by comparison with the *Bacillus pasteurii* cyt c (Bp cyt *c*) to the Ht protein. In the Bp cytochrome, the Met-Fe interaction is extremely stable under a vast pH range, and upon the loss of the axial ligation, the protein totally unfolds.[82] In terms of sequence, the Met-bearing loop of the Bp protein is 9 amino acids in length and rich in Gly and Pro residues, a combination of factors that yield a very

rigid structure.[82] The Met-donating loop found in the Ht cytochrome is also rich in Gly and Pro: it contains four Gly residues throughout the first half of the loop, and three Pro residues, which flank the axial Met. However, the loop is larger, 17 amino acids, and the increases size may decrease the overall energy barrier for the isomerization required for the Met-loss process studied here.[16]

The question remains: following the Met-loss process, what is the nature of the new ligand, if any? Notably, the data presented here for the M61A mutant indicate that the Met loss state likely includes a protein-based ligand in the distal position. In terms of potential ligands, there are no other His present in the Ht *cyt* c sequence, but the closest available lysine residues (K49 and K50) are homologous to K72/K73 of mitochondrial cyts *c* (where K73 is known to participate in formation of the alkaline conformer along with K79,[28-30] which is not a conserved lysine in the Ht protein). K49 and K50 are at the terminus of helix three, where they participate in hydrogen bonding,[16] while helix three also has residues that contribute to the hydrophobic core of the protein, playing a key role in protein folding.[16,81] In the homologous Pa cyt *c* helix three and the Met-donating loop are known to exist within the same foldon, displaying a free energy of unfolding of 26-34 kJ mol^{-1}.[81] While identical data is not available for Ht, the lower free energy reported her may represent the unfolding and ligand rearrangement of a smaller element of structure, or an overall decrease of the necessary driving force, due to the interaction with the electrode. Either way, similarities in structure suggest that *partial* unfolding of helix three may not totally perturb the whole structure due to normal solution dynamics.[74] Thus, we hypothesize that the ΔG_{ML} for the Met-loss transformation reported here may be concomitant with localized helix fraying, in which one of the terminal Lys residues of helix three binds at the newly available coordination site, in a manner that is exchangeable with Im. Notably, the Met-loss form observed here and elsewhere is somewhat higher in potential (~ -100 mV at pH 6.0) than the "alkaline conformers" of forms of yeast iso-1-cytochrome *c* reported by Rosell and co-workers (-160 to -170 mV at pH 6.0), where the difference of 50 mV may be due to lingering differences in solvent exposure or due to the binding energy of the PGE surface. Regardless of the basis of the change, validating this hypothesis with electrochemically-poised spectroscopies will be an ongoing research effort in the future.

CONCLUSIONS

In conclusion, we have begun to elucidate the nature of the Met-loss feature exhibited by Ht cyt c_{552} on PGE electrodes. We have shown that the Ht cyt *c* is susceptible to ligand replacement by the small molecule imidazole. The imidazole-cyt *c* adduct is similar to the low potential Met-loss feature initially associated with PGE surface. And similarly mutations to Met61 can be made to mimic that of the low potential form in the presence of an imidazole ligand (His based or extrinsic). Redox thermodynamics associated with the normal and alkaline forms of WT, M61A, and M61H Ht cytochromes are consistent with those from other species. Finally the required driving force for reorganization of Ht cyt *c* Met-bearing loop is lowered by the PGE surface, displaying an equilibrium that can be readily enhanced at modest, yet elevated temperatures. The conformational change may be physiological, however the impact may be dictated by the local versus global stability associated with the Met-donating loops.

Supplementary Material

Refer to Web version on PubMed Central for supplementary material.

Acknowledgments

The authors gratefully acknowledge the generous support of the National Science Foundation (grant MCB546323, S.J.E.) and the National Institutes of Health (grant R01-GM63170, K.L.B. and grant R01-GM72663).

REFERENCES

1. Bertini I, Cavallaro G, Rosato A. Chem. Rev. 2006; 106:90–115. [PubMed: 16402772]
2. Marcus RA, Sutin N. Biochim. Biophys. Acta. 1985; 811:265–322.
3. Paoli M, Marles-Wright J, Smith A. DNA Cell. Biol. 2002; 21:271–280. [PubMed: 12042067]
4. Winkler JR. Curr. Opin. Chem. Biol. 2004; 8:169–174. [PubMed: 15062778]
5. Tezcan FA, Winkler JR, Gray HB. J. Am. Chem. Soc. 1998; 120:13383–13388.
6. Bixler J, Bakker G, McLendon G. J. Am. Chem. Soc. 1992; 114:6938–6939.
7. Gunner MR, Honig B. Proc. Natl. Acad. Sci. U.S.A. 1991; 88:9151–9155. [PubMed: 1924378]
8. Moore, GR.; Pettigrew, GW. Cytochromes c : evolutionary, structural, and physicochemical aspects. Springer-Verlag; New York: 1990. p. 66-209.
9. Mao JJ, Hauser K, Gunner MR. Biochemistry. 2003; 42:9829–9840. [PubMed: 12924932]
10. Scott, RA.; Mauk, AG. Cytochrome C : a multidisciplinary approach. University Science Books; Sausalito, California: 1996. p. 3-103.
11. Bowman SEJ, Bren KL. Inorg. Chem. 2010; 49:7890–7897. [PubMed: 20666367]
12. Michel LV, Ye T, Bowman SEJ, Levin BD, Hahn MA, Russell BS, Elliott SJ, Bren KL. Biochemistry. 2007; 46:11753–11760. [PubMed: 17900177]
13. Ye T, Kaur R, Senguen FT, Michel LV, Bren KL, Elliott SJ. J. Am. Chem. Soc. 2008; 130:6682–6683. [PubMed: 18454519]
14. Ye T, Kaur R, Wen X, Bren KL, Elliott SJ. Inorg. Chem. 2005; 44:8999–9006. [PubMed: 16296855]
15. Wen X, Patel KM, Russell BS, Bren KL. Biochemistry. 2007; 46:2537–2544. [PubMed: 17279778]
16. Travaglini-Allocatelli C, Gianni S, Dubey VK, Borgia A, Di Matteo A, Bonivento D, Cutruzzola F, Bren KL, Brunori M. J. Biol. Chem. 2005; 280:25729–25734. [PubMed: 15883159]
17. Russell BS, Bren KL. J. Biol. Inorg. Chem. 2002; 7:909–916. [PubMed: 12203029]
18. Russell BS, Melenkivitz R, Bren KL. Proc. Natl. Acad. Sci. U.S.A. 2000; 97:8312–8317. [PubMed: 10880578]
19. Wen X, Bren KL. Inorg. Chem. 2005; 44:8587–8593. [PubMed: 16271000]
20. Wen X, Bren KL. Biochemistry. 2005; 44:5225–5233. [PubMed: 15794659]
21. Zhong LH, Wen X, Rabinowitz TM, Russell BS, Karan EF, Bren KL. Proc. Natl. Acad. Sci. U.S.A. 2004; 101:8637–8642. [PubMed: 15161973]
22. Paes de Sousa PM, Pauleta SR, Simões Gonçalves ML, Pettigrew GW, Moura I, Correia dos Santos MM, Moura JJG. J. Biol. Inorg. Chem. 2007; 12:691–698. [PubMed: 17361419]
23. Banci L, Bertini I, Liu GH, Lu J, Reddig T, Tang WX, Wu YB, Yao Y, Zhu DX. J. Biol. Inorg. Chem. 2001; 6:628–637. [PubMed: 11472026]
24. Battistuzzi G, Borsari M, Cowan JA, Ranieri A, Sola M. J. Am. Chem. Soc. 2002; 124:5315–5324. [PubMed: 11996572]
25. Battistuzzi G, Borsari M, De Rienzo F, Di Rocco G, Ranieri A, Sola M. Biochemistry. 2007; 46:1694–1702. [PubMed: 17243773]
26. Barker PD, Mauk AG. J. Am. Chem. Soc. 1992; 114:3619–3624.
27. Dopner S, Hildebrandt P, Rosell FI, Mauk AG. J. Am. Chem. Soc. 1998; 120:11246–11255.
28. Ferrer JC, Guillemette JG, Bogumil R, Inglis SC, Smith M, Mauk AG. J. Am. Chem. Soc. 1993; 115:7507–7508.
29. Pollock WBR, Rosell FI, Twitchett MB, Dumont ME, Mauk AG. Biochemistry. 1998; 37:6124–6131. [PubMed: 9558351]
30. Rosell FI, Ferrer JC, Mauk AG. J. Am. Chem. Soc. 1998; 120:11234–11245.

31. Creutz C, Sutin N. J. Biol. Chem. 1974; 249:6788–6795. [PubMed: 4371651]
32. Schejter A, Aviram I. Biochemistry. 1969; 8:149–153. [PubMed: 5777317]
33. Schejter A, Plotkin B, Vig I. Febs Lett. 1991; 280:199–201. [PubMed: 1849482]
34. Schejter A, Ryan MD, Blizzard ER, Zhang CY, Margoliash E, Feinberg BA. Protein Sci. 2006; 15:234–241. [PubMed: 16434742]
35. Viola F, Aime S, Coletta M, Desideri A, Fasano M, Paoletti S, Tarricone C, Ascenzi P. J. Inorg. Biochem. 1996; 62:213–222. [PubMed: 8627283]
36. Assfalg M, Bertini I, Dolfi A, Turano P, Mauk AG, Rosell FI, Gray HB. J. Am. Chem. Soc. 2003; 125:2913–2922. [PubMed: 12617658]
37. Dumortier C, Meyer TE, Cusanovich MA. Arch. Biochem. Biophys. 1999; 371:142–148. [PubMed: 10545200]
38. Spooner PJR, Watts A. Biochemistry. 1991; 30:3871–3879. [PubMed: 1850290]
39. Spooner PJR, Watts A. Biochemistry. 1991; 30:3880–3885. [PubMed: 1850291]
40. Dumortier C, Fitch J, Meyer TE, Cusanovich MA. Arch. Biochem. Biophys. 2002; 405:154–162. [PubMed: 12220527]
41. Dumortier C, Fitch J, Van Petegem F, Vermulen W, Meyer TE, Van Beeumen JJ, Cusanovich MA. Biochemistry. 2004; 43:7717–7724. [PubMed: 15196014]
42. Dumortier C, Holt JM, Meyer TE, Cusanovich MA. J. Biol. Chem. 1998; 273:25647–25653. [PubMed: 9748230]
43. Spooner PJR, Duralski AA, Rankin SE, Pinheiro TJT, Watts A. Biophys. J. 1993; 65:106–112. [PubMed: 8396450]
44. Spooner PJR, Watts A. Biochemistry. 1992; 31:10129–10138. [PubMed: 1327134]
45. Basova LV, Kurnikov IV, Wang L, Ritov VB, Belikova NA, Vlasova II, Pacheco AA, Winnica DE, Peterson J, Bayir H, Waldeck DH, Kagan VE. Biochemistry. 2007; 46:3423–3434. [PubMed: 17319652]
46. Battistuzzi G, Borsari M, Loschi L, Martinelli A, Sola M. Biochemistry. 1999; 38:7900–7907. [PubMed: 10387031]
47. Battistuzzi G, Borsari M, Ranieri A, Sola M. Arch. Biochem. Biophys. 2002; 404:227–233. [PubMed: 12147260]
48. Tai HL, Nagatomo S, Mita H, Sambongi Y, Yamamoto YB. Chem. Soc. Jpn. 2005; 78:2019–2025.
49. Terui N, Tachiiri N, Matsuo H, Hasegawa J, Uchiyama S, Kobayashi Y, Igarashi Y, Sambongi Y, Yamamoto Y. J. Am. Chem. Soc. 2003; 125:13650–13651. [PubMed: 14599189]
50. Yamamoto Y, Terui N, Tachiiri N, Minakawa K, Matsuo H, Kameda T, Hasegawa J, Sambongi Y, Uchiyama S, Kobayashi Y, Igarashi Y. J. Am. Chem. Soc. 2002; 124:11574–11575. [PubMed: 12296704]
51. Harbury HA, Cronin JR, Fanger MW, Hettinge TP, Murphy AJ, Myer YP, Vinograd SN. Proc. Natl. Acad. Sci. U.S.A. 1965; 54:1658–1664. [PubMed: 5218919]
52. Battistuzzi G, Borsari M, Cowan JA, Eicken C, Loschi L, Sola M. Biochemistry. 1999; 38:5553–5562. [PubMed: 10220343]
53. Battistuzzi G, Borsari M, Sola M, Francia F. Biochemistry. 1997; 36:16247–16258. [PubMed: 9405059]
54. Taniguchi VT, Sailasutascott N, Anson FC, Gray HB. Pure Appl. Chem. 1980; 52:2275–2281.
55. Tai HL, Mikami S, Irie K, Watanabe N, Shinohara N, Yamamoto Y. Biochemistry. 2010; 49:42–48. [PubMed: 19947659]
56. Ho SN, Hunt HD, Horton RM, Pullen JK, Pease LR. Gene. 1989; 77:51–59. [PubMed: 2744487]
57. Arslan E, Schulz H, Zufferey R, Kunzler P, Thony-Meyer L. Biochem. Bioph. Res. Co. 1998; 251:744–747.
58. Massari AM, Finkelstein IJ, McClain BL, Goj A, Wen X, Bren KL, Loring RF, Fayer MD. J. Am. Chem. Soc. 2005; 127:14279–14289. [PubMed: 16218622]
59. Karan EF, Russell BS, Bren KL. J. Biol. Inorg. Chem. 2002; 7:260–272. [PubMed: 11935350]
60. Fourmond V, Hoke K, Heering HA, Baffert C, Leroux F, Bertrand P, Leger C. Bioelectrochemistry. 2009; 76:141–147. [PubMed: 19328046]

61. Leger C, Bertrand P. Chem. Rev. 2008; 108:2379–2438. [PubMed: 18620368]
62. Sutin N, Yandell JK. J. Biol. Chem. 1972; 247:6932–6936. [PubMed: 4343163]
63. Gianni S, Travaglini-Allocateli C, Cutruzzolla F, Brunori M, Shastry MCR, Roder H. J. Mol. Biol. 2003; 330:1145–1152. [PubMed: 12860134]
64. Pulcu GS, Elmore BL, Arciero DM, Hooper AB, Elliott SJ. J. Am. Chem. Soc. 2007; 129:1838–1839. [PubMed: 17263529]
65. Reedy CJ, Gibney BR. Chem. Rev. 2004; 104:617–649. [PubMed: 14871137]
66. Raphael AL, Gray HB. J. Am. Chem. Soc. 1991; 113:1038–1040.
67. Anderson JLR, Chapman SK. Dalton Trans. 2005; (1):13–24. [PubMed: 15605142]
68. Marques HM. Dalton Trans. 2007; (39):4371–4385. [PubMed: 17909648]
69. Battistuzzi G, Borsari M, Di Rocco G, Ranieri A, Sola M. J. Biol. Inorg. Chem. 2004; 9:23–26. [PubMed: 14586786]
70. Lin J, Breck WG. Can. J. Chem. 1965; 43:766–771.
71. Yee EL, Cave RJ, Guyer KL, Tyma PD, Weaver MJ. J. Am. Chem. Soc. 1979; 101:1131–1137.
72. Takahashi YT, Sasaki H, Takayama SIJ, Mikami SI, Kawano S, Mita H, Sambongi Y, Yamamoto Y. Biochemistry. 2006; 45:11005–11011. [PubMed: 16953587]
73. Uchiyama S, Ohshima A, Nakamura S, Hasegawa J, Terui N, Takayama SIJ, Yamamoto Y, Sambongi Y, Kobayashi Y. J. Am. Chem. Soc. 2004; 126:14684–14685. [PubMed: 15535669]
74. Englander SW, Mayne L, Krishna MMG. Q. Rev. Biophys. 2007; 40:287–326. [PubMed: 18405419]
75. Winzor DJ, Jackson CM. J. Mol. Recognit. 2006; 19:389–407. [PubMed: 16897812]
76. Bai YW, Milne JS, Mayne L, Englander SW. Proteins Struct. Funct. Genet. 1994; 20:4–14. [PubMed: 7824522]
77. Bai YW, Sosnick TR, Mayne L, Englander SW. Science. 1995; 269:192–197. [PubMed: 7618079]
78. Englander SW, Mayne L, Rumbley JN. Biophys. Chem. 2002; 101:57–65. [PubMed: 12487989]
79. Krishna MMG, Maity H, Rumbley JN, Englander SW. Protein Sci. 2007; 16:1946–1956. [PubMed: 17660254]
80. Krishna MMG, Maity H, Rumbley JN, Lin Y, Englander SW. J. Mol. Biol. 2006; 359:1410–1419. [PubMed: 16690080]
81. Michel LV, Bren KL. J. Biol. Inorg. Chem. 2008; 13:837–845. [PubMed: 18392863]
82. Bartalesi I, Bertini I, Di Rocco G, Ranieri A, Rosato A, Vanarotti M, Vasos PR, Viezzoli MS. J. Biol. Inorg. Chem. 2004; 9:600–608. [PubMed: 15175936]

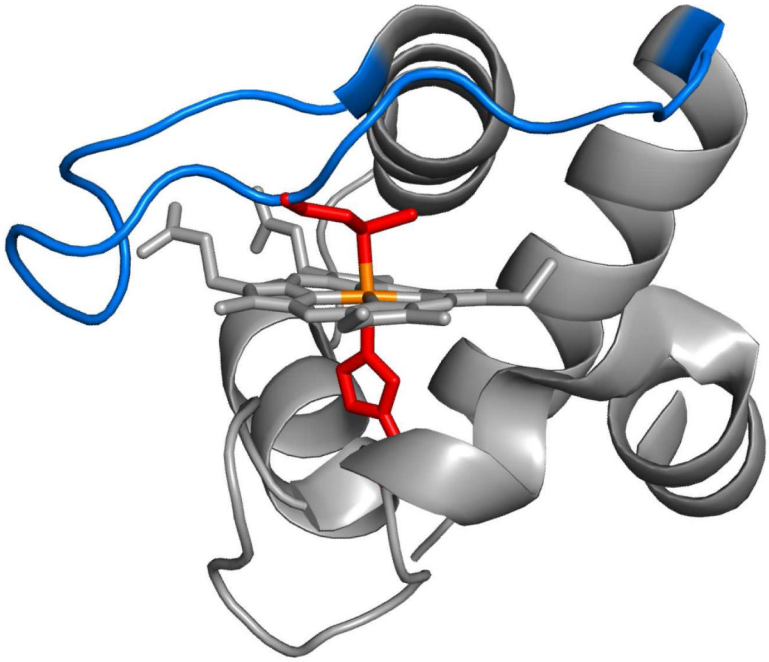

FIGURE 1.

Cartoon representation of HT cyt c_{552} constructed from Protein Data Bank ID:1YNR[16] utilizing PyMOL. The heme *c* and axial ligands, His16 and Met61, are displayed as sticks. Axial ligands His16 (bottom) and Met61 (top) are highlighted in red. The Met-donating loop, loop3 is highlighted in blue.

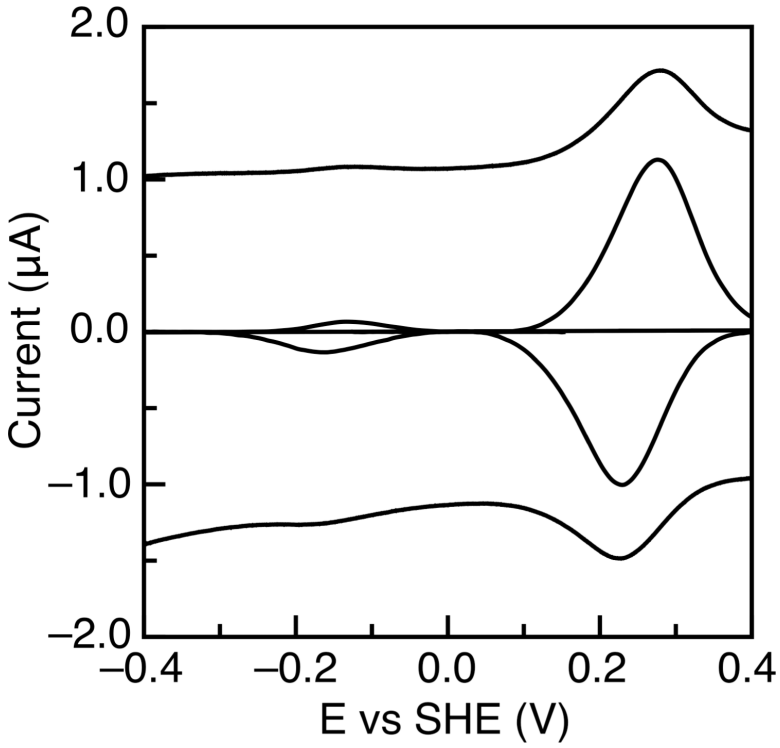

FIGURE 2.

Representative data for typical PFV experiments utilizing PGE electrodes for HT WT. The raw data is shown as the solid black line. The non-faradaic current was removed and is shown inset. 50 mM MOPS buffer pH 6.0, 200 mM NaCl, 5 °C, and scan rate = 200 mV/s.

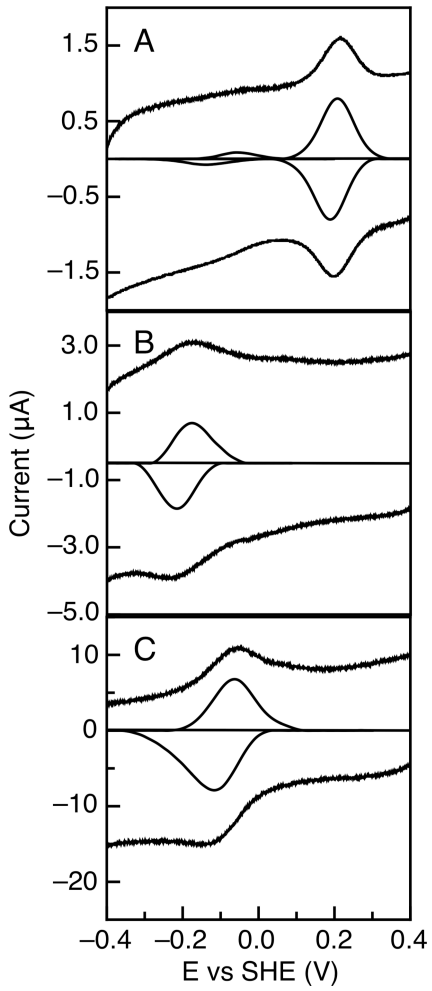

FIGURE 3.

PFV response for (A) HT WT cyt c_{552} (B) HT M61A (C) HT M61H upon PGE electrodes. Raw data are shown, and the non-faradaic portion of the current was subtracted, resulting in the data shown inset into each panel. All data were collected in 50 mM phosphate/citrate buffer pH 6.0, 200 mM NaCl, 0 °C, and scan rate = 200 mV/s.

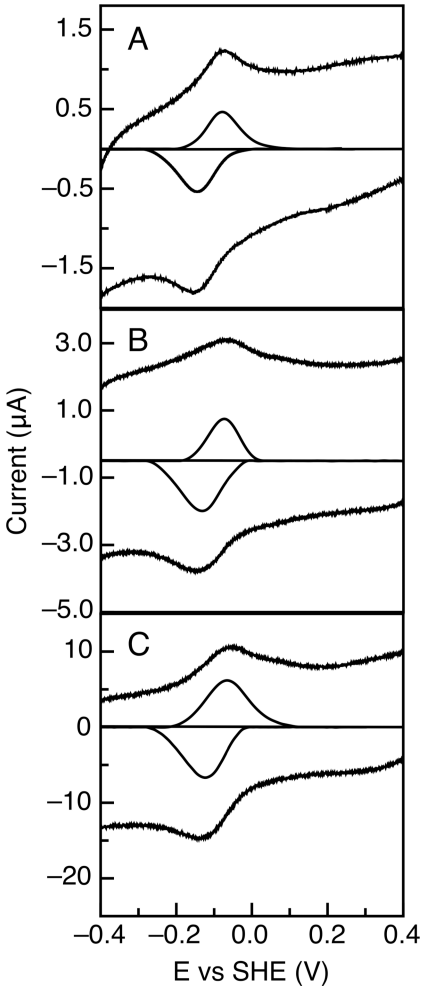

FIGURE 4.

Effect of imidazole binding on the relative electrochemical populations of bound states upon PGE electrodes. (A) HT WT cyt c_{552} (B) HT M61A (C) HT M61H. All data were collected in 50 mM phosphate/citrate buffer pH 6.0, 200 mM NaCl, 0 °C, 750 mM imidazole, and scan rate = 200 mV/s.

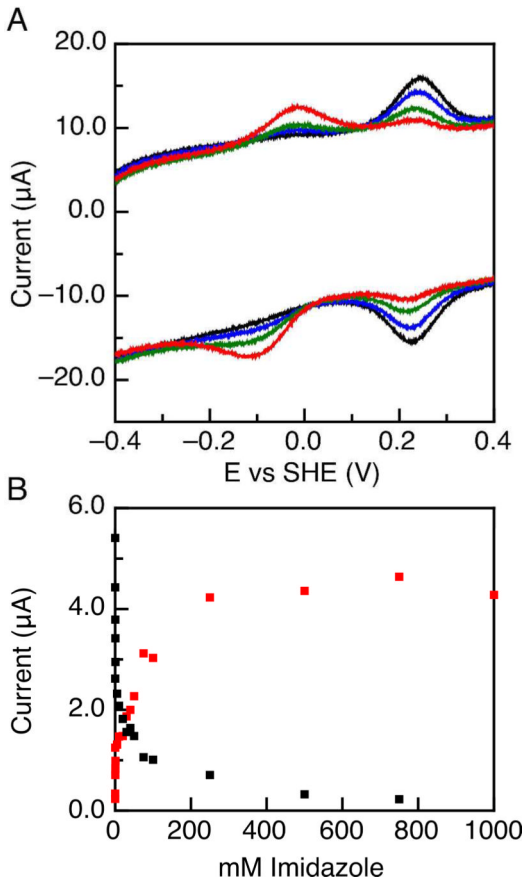

FIGURE 5.

(A) Cyclic voltammograms of HT WT from 0 – 100 mM imidazole. All data was collected in 50 mM phosphate/citrate buffer pH 6.0, 200 mM NaCl, 0 °C, and scan rate = 200 mV/s. (B) Change in the cathodic current intensity of the Normal (Black) and Met-loss (Red) form of HT WT as a function of imidazole concentration. Anodic current (not shown) behaves in a similar manner.

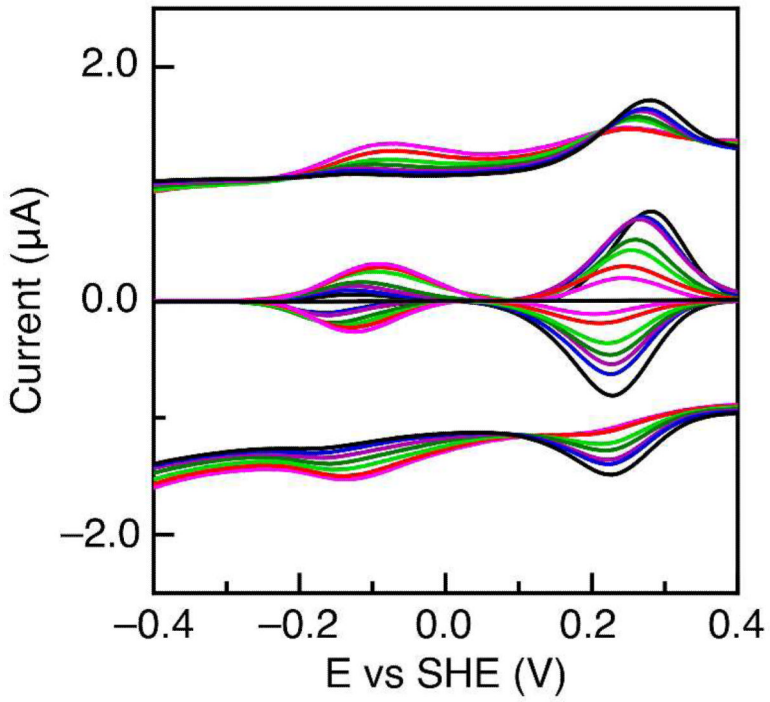

FIGURE 6.

Variable temperature PFV response of HT WT. The initial films were generated upon PGE electrodes at 276 K (black). Subsequently the temperature was warmed to 278 (brown), 288 (blue), 298 (purple), 308 (dark green), 318 (light green), 328 (red), and 338 K (pink). All data was collected in 50 mM MOPS pH 7.0.

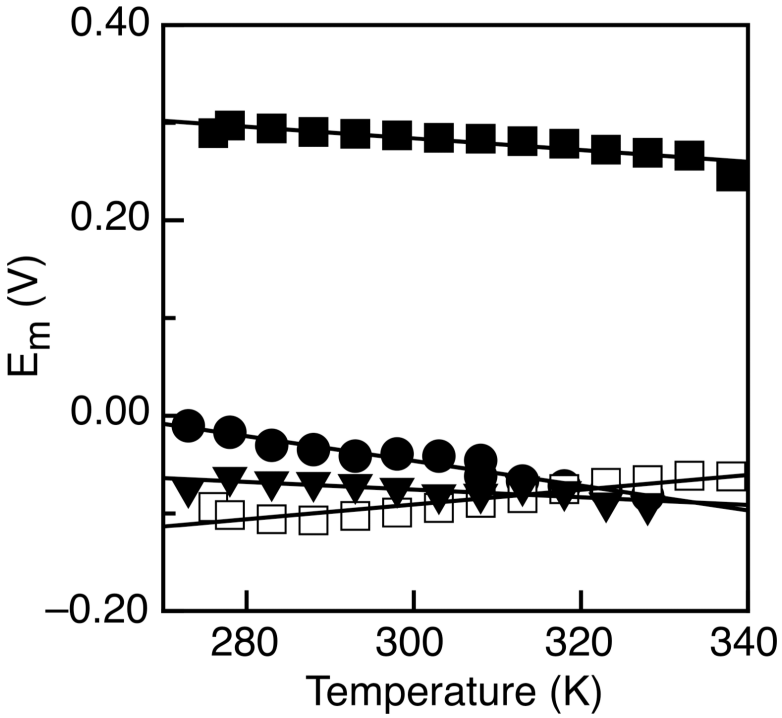

FIGURE 7.

E_m vs T plot for HT WT (■) normal and (□) Met-loss, (□) HT M61A, and (•) HT M61H. Data is fit to a linear regression model where the slope = $\Delta S/nF$, where n = $1e^-$, and shown in the solid black lines.

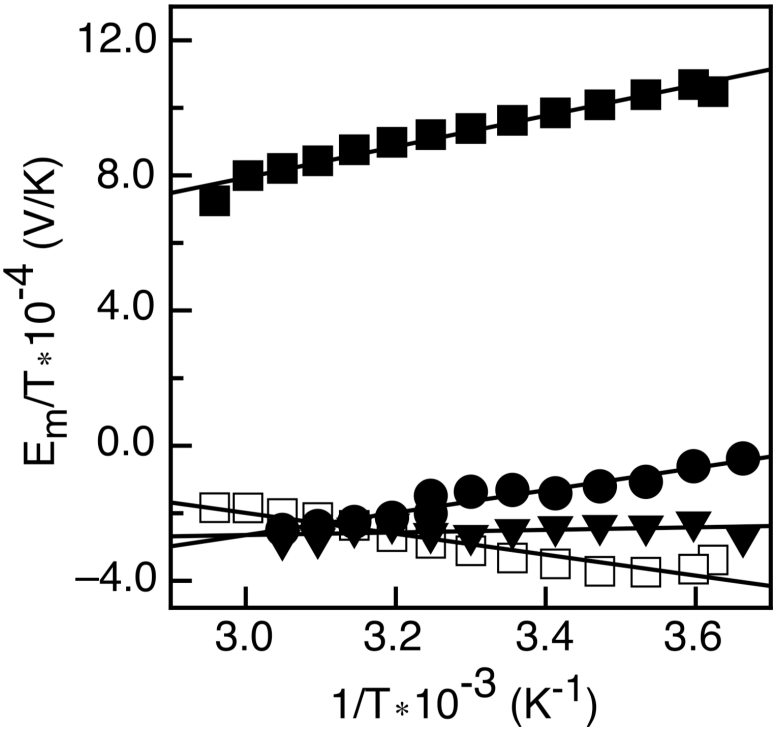

FIGURE 8.

Gibb-Helmoltz plot of HT WT (■) normal and (□) Met-loss forms, (□) HT M61A, and (•) HT M61H. Linear regression analysis was used to fit each data set and extract the redox enthalpy. Fits are shown in solid black lines.

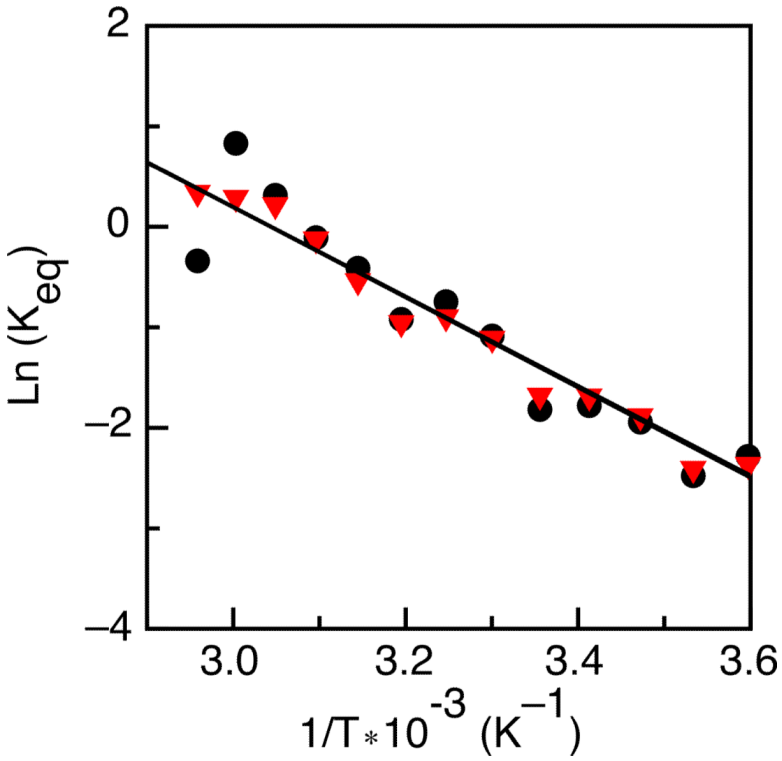

FIGURE 9.

Plot of ln(K_{eq}) vs 1/T used to determine the Gibbs free energy of Met61 loss. The equilibrium constant (K_{eq}) was determined by (●) peak area and (▼) peak intensity. Linear regression analysis was used to fit each data set and are shown by the solid line.

Table 1

Midpoint Potentials determined for the normal and imidazole bound features of Ht cytochrome *c*.

Protein	E_m vs SHE (mV)	
	Normal[a]	+Imidazole[b]
HT WT[c]	+210 ± 2	-110 ± 3
HT M61H	-103 ± 2	-103 ± 2
HT M61A	-163 ± 2	-69 ± 2

[a] The normal, high potential couple, observed in the absence of non-native coordinating ligand.

[b] The low potential feature populated by the addition of imidazole.

[c] These additionally correspond to the reduction potentials normal and “met-loss” form of Ht WT in the absence of imidazole.

Table 2

Thermodynamic parameters determined for the native and mutant forms of Ht cytochrome *c* determined by variable temperature PFV.

Protein	$\Delta S°'_{rc}$ J K^{-1} mol^{-1}	$\Delta H°'_{rc}$ kJ mol^{-1}	$\Delta S°'_{ML}$ [b] J K^{-1} mol^{-1}	$\Delta H°'_{ML}$ [b] kJ mol^{-1}
WT	-49.1	-42.2	95.7	36.7
M61H	-127.0	-31.1		
M61A	-56.2	-3.7		

[a] The average errors for ΔH°' and AS°' are ± 3 kJ mol^{-1} and ± 6 J $K^{-1}$$mol^{-1}$ respectively.

[b] Met-loss form.

Table 3

Comparison of Gibbs free energy for the Met-loss form (ML), sub-global hydrogen exchange of the methionine donating loop (HX), and mitochondrial alkaline form (AT).

Species	$\Delta G_{ML,\ 273\ K}$	ΔG_{HX}	ΔG_{AT}
	kJ mol^{-1}	**kJ mol^{-1}**	**kJ mol^{-1}**
Ht cyt c_{552}[a]	6.3		
Pa cyt c_{551}[b]		26 - 34	
Hh cyt c[c]		26.3	
Beef heart cyt c[d]			52
YCC[e]			48

[a] Error for both the upper and lower bounds are ± 0.2 KJ mol^{-1}

[b] Ref. 81

[c] Ref. 80

[d] Ref. 46

[e] Ref. 47.